TBX1 regulates chondrocyte maturation in the spheno-occipital synchondrosis

Noriko Funato et al.

Appendix

Appendix Table 1. Tissue-Specific Deletion of *Tbx1* with the Indicated Cre Driver to Determine the Causative Tissue for the Synchondrosis Phenotype Observed in *Tbx1*$^{-/-}$ Mice.

	Tbx1$^{+/-}$	*Tbx1*$^{-/-}$	*Tbx1*$^{loxP/+}$	*Tbx1*$^{KO/loxP}$; *Mesp1-Cre*	*Tbx1*$^{KO/loxP}$; *Twist2-Cre*	*Tbx1*$^{KO/loxP}$; *Wnt1-Cre*	*Tbx1*$^{KO/loxP}$; *KRT14-Cre*
Cell type				**Mesodermal cells**	**Osteochondral progenitors**	**Neural crest cells**	**Keratinocytes**
FACE							
Cranium	–	brachycephaly	–	brachycephaly	brachycephaly	–	–
	(n=9)	100% (5/5)	(n=11)	100% (3/3)	100% (8/8)	(n=6)	(n=5)
Ear	–	Low-set	–	Low-set	Low-set	–	–
	(n=9)	100% (5/5)	(n=11)	100% (3/3)	100% (8/8)	(n=6)	(n=5)
Pinna	–	small	–	small	–	–	–
	(n=9)	100% (5/5)	(n=11)	100% (3/3)	(n=8)	(n=6)	(n=5)
CRANIAL BASE							
Intersphenoid synchondrosis	–	–	–	–	–	–	–
	(n=9)	(n=5)	(n=11)	(n=3)	(n=8)	(n=6)	(n=5)
Presphenoid synchondrosis	–	–	–	–	–	–	–
	(n=9)	(n=5)	(n=11)	(n=3)	(n=8)	(n=6)	(n=5)
Spheno-occipital synchondrosis	–	complete fusion	–	complete fusion	partial fusion	–	–
	(n=9)	100% (5/5)	(n=11)	100% (3/3)	100% (8/8)	(n=6)	(n=5)
Basisphenoid bone	–	hypoplastic malformed	–	malformed	malformed	–	–
	(n=9)	100% (5/5)	(n=11)	100% (3/3)	100% (8/8)	(n=6)	(n=5)
Basioccipital bone	–	hypoplastic malformed	–	malformed	malformed	–	–
	(n=9)	100% (5/5)	(n=11)	100% (3/3)	100% (8/8)	(n=6)	(n=5)

Appendix Table 2. Mouse Genes Involved in Embryonic Development of the Spheno-Occipital Synchondrosis.

Gene	Protein	Synchondrosis	Mouse Age	References
Chrd	chordin	SOS	P1	*Development.* 2003; 130(15):3567-3578.
Ctnnb1	catenin beta 1	SOS	E18.5	*Dev Biol.* 2011; 349(2):261-269.
Fgfr2	fibroblast growth factor receptor 2	SOS	P1	*Bone.* 2011; 48(4):847-856.
Fgfrl1	fibroblast growth factor receptor like 1	SOS	E18.5	*Dis Model Mech.* 2009; 2(5-6):283-294.
Ihh	indian hedgehog	SOS	E18.5	*J Pathol.* 2005; 207(4):453-461.
Lef1	lymphoid enhancer binding factor 1	ISS, SOS	E17.5	*J Dent Res.* 2008; 87(3):244-249.
Mef2c	myocyte enhancer factor 2C	SOS	E18.5	*Dev Cell.* 2007; 12:377–389.
Pth1r	parathyroid hormone 1 receptor	SOS	E18.5	*Science.* 1996; 273(5275):663-666.
Pthlh (Pthrp)	parathyroid hormone-like peptide	ISS, SOS	P1	*Anat Rec.* 1999; 255(4):452-457.
Runx2	runt related transcription factor 2	ISS, SOS	P1	*Genes Dev.* 2001; 15(4):467-481.
Six2	sine oculis-related homeobox 2	ISS, SOS	P1	*Dev Biol.* 2010; 344(2):720-730.
Six1	sine oculis-related homeobox 1	SOS	E18.5	*Dev Biol.* 2010; 344(2):720-730.
Six4	sine oculis-related homeobox 4	SOS	E18.5	*Dev Biol.* 2010; 344(2):720-730.
Tbx1	T-box 1	SOS	E15.5	This paper

SOS, spheno-occipital synchondrosis; ISS, intersphenoid synchondrosis.

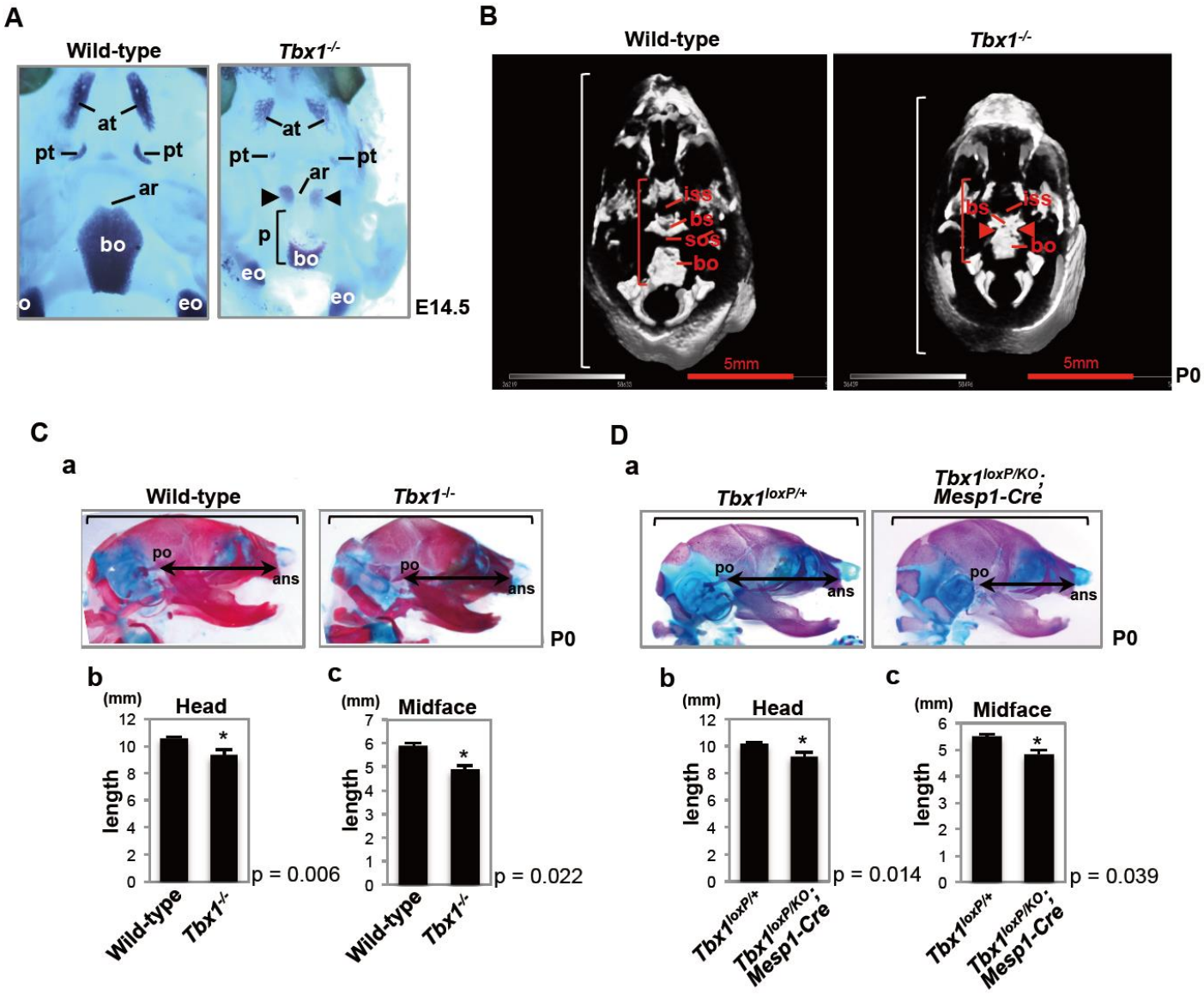

Appendix Figure 1. *Tbx1*$^{-/-}$ mice show craniofacial deformities.

(A) Alizarin red and Alcian blue staining of cranial bases from wild-type and *Tbx1*$^{-/-}$ mice at embryonic day (E)14.5. Precocious ossification (arrowheads) was detected in the acrochordal cartilage (ar) of *Tbx1*$^{-/-}$ embryos.

(B) Skulls from wild-type and *Tbx1*$^{-/-}$ mice at postnatal day (P) 0 were analyzed by micro-computed tomography (μCT) and are shown in a 'bird's eye view'. The basisphenoid (bs) and basioccipital (bo) bones are fused (arrowheads). The length of head (white brackets) and the cranial base (red brackets) in *Tbx1*$^{-/-}$ mice are much shorter than those in wild-type.

(C) Alizarin red and Alcian blue staining (a) of head from wild-type and *Tbx1*$^{-/-}$ mice at P0. The head length (brackets) and the midface length (arrows) in wild-type (n = 3) and *Tbx1*$^{-/-}$ mice (n = 3) were measured and evaluated (b, c). The data represent the mean ± s.e.m. **P* < 0.05.

(D) Alizarin red and Alcian blue staining (a) of head from control *Tbx1*$^{loxP/+}$ and *Tbx1*$^{loxP/KO}$; *Mesp1-Cre* mice at P0. The head length (brackets) and the midface length (arrows) in wild-type (n = 3) and *Tbx1*$^{loxP/KO}$; *Mesp1-Cre* mice (n = 3) were measured and evaluated (b, c). The data represent the mean ± s.e.m. **P* < 0.05.

po, porion; ans, anterior nasal spine; bo, basioccipital bone; p, parachordal cartilage; at, ala temporalis (greater wing) of the basisphenoid bone; pt, pterygoid bone; eo, exoccipital bone; sos, spheno-occipital synchondrosis; iss, intersphenoid synchondrosis.

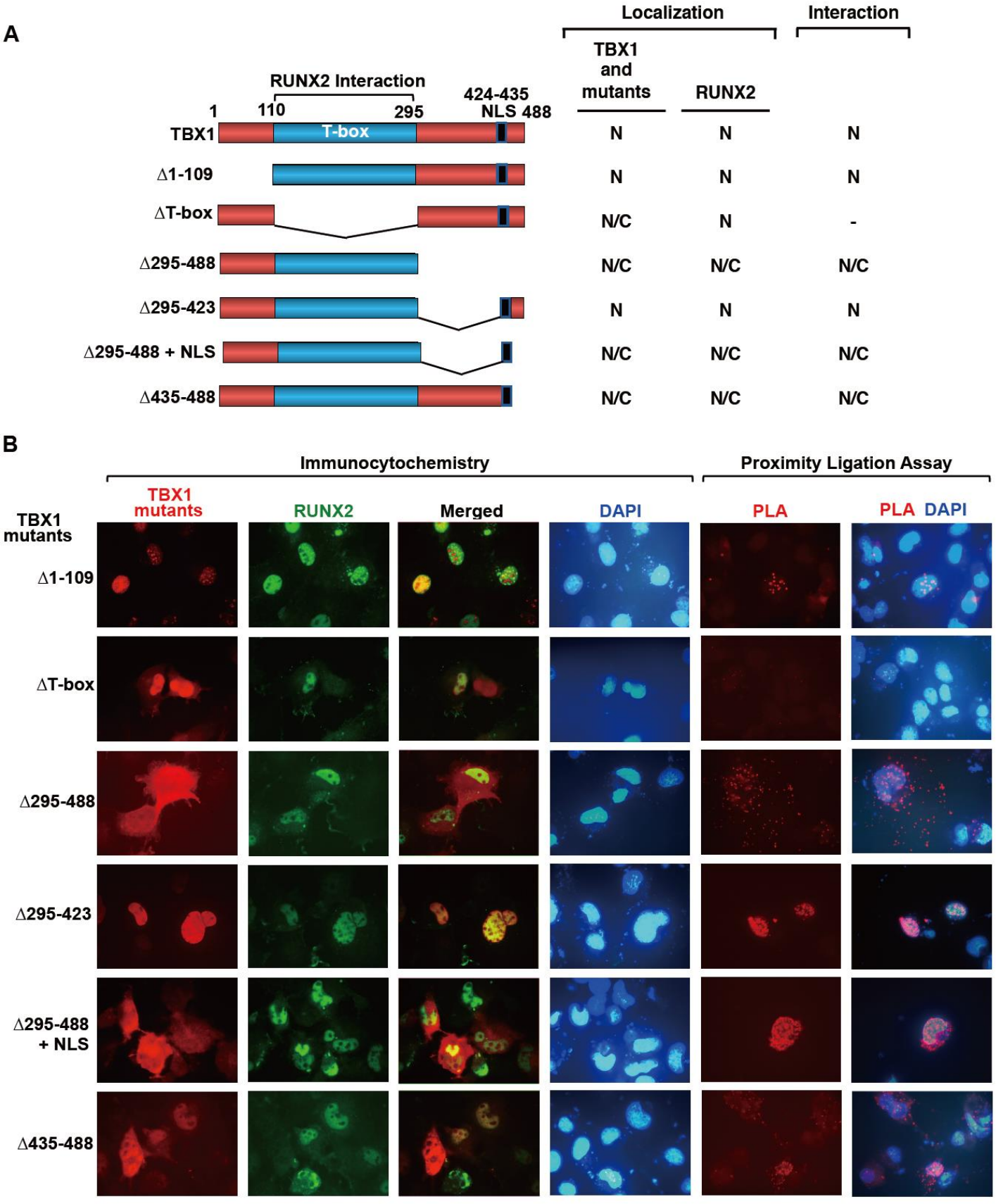

Appendix Figure 2. TBX1 Affects RUNX2 Localization.

(A) Schematic representation of TBX1 functional domains and deletion mutants. All constructs contained an N-terminal Myc-epitope-tag. TBX1 functionally interacts with RUNX2 via the T-box domain. NLS, nuclear localization signal; N, nucleus; N/C, nucleus and cytoplasm.

(B) Subcellular localization (immunocytochemistry) and *in situ* proximity ligation assay (PLA) of Flag-tagged RUNX2 and Myc-tagged TBX1 mutants using anti-Myc and anti-Flag antibodies. COS-1 cells were transfected with Myc-TBX1 deletion mutants and Flag-RUNX2. Protein–protein interactions between TBX1 deletion mutants and RUNX2 were assessed by PLA. The detected interaction sites are marked by fluorescent dots (red); nuclei were counterstained with 4′,6′-diamidino-2-phenylindole (DAPI; blue).

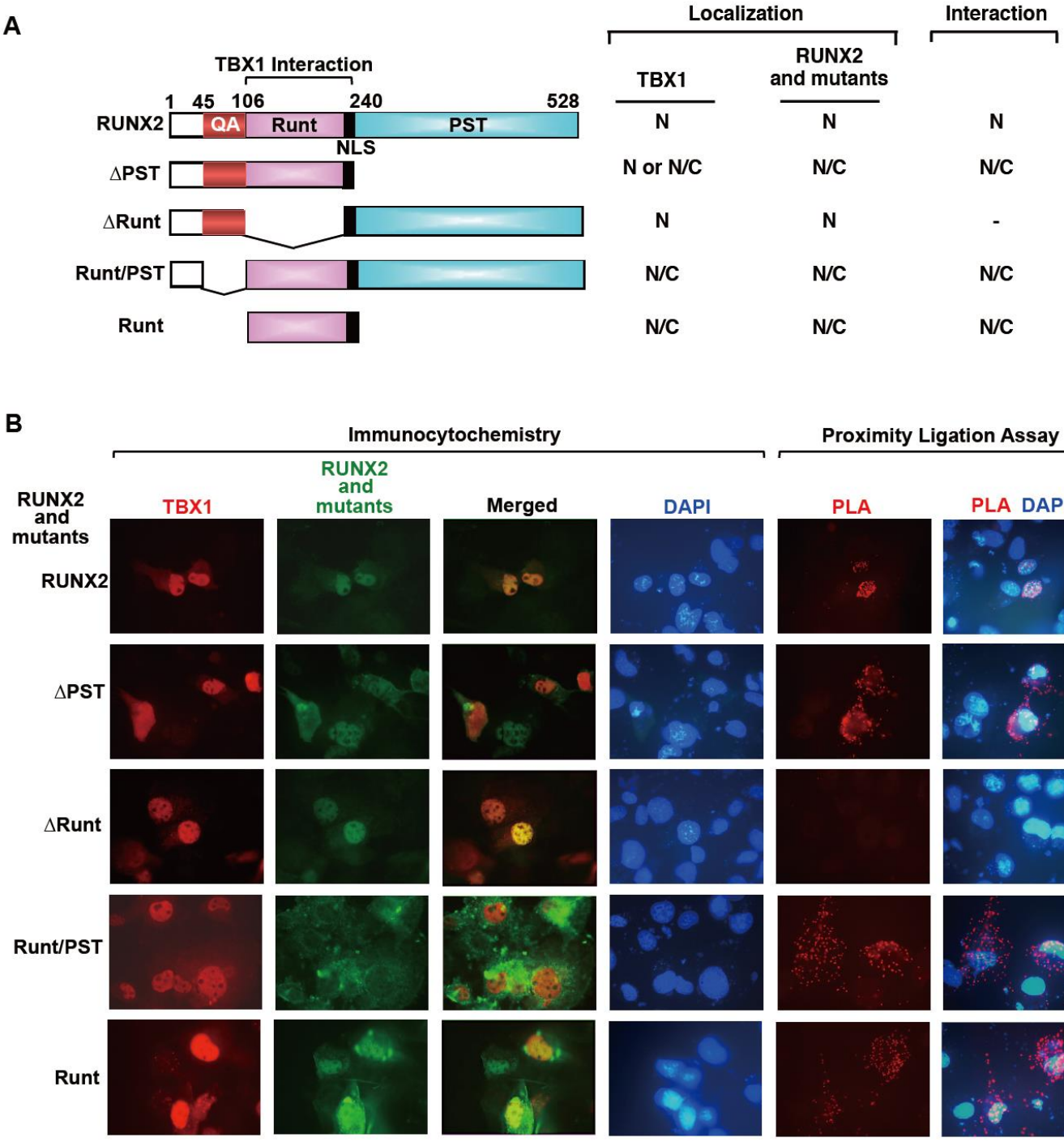

Appendix Figure 3. RUNX2 Affects TBX1 Localization.

(A) Schematic representation of RUNX2 deletion mutants and functional domains. All constructs contained an N-terminal Flag-epitope-tag. RUNX2 functionally interacts with TBX1 via the Runt domain. Runt, runt DNA-binding domain; QA, glutamine/alanine repeats; PST, proline/serine/threonine-rich region; NLS, nuclear localization signal; N, nucleus; N/C, nucleus and cytoplasm.

(B) Subcellular localization (immunocytochemistry) and *in situ* proximity ligation assay (PLA) of Myc-tagged TBX1 and Flag-tagged RUNX2 mutants using anti-Myc and anti-Flag antibodies. COS-1 cells were transfected with Myc-TBX1, Flag-RUNX2, or Flag-RUNX2 deletion mutants. Protein–protein interactions between TBX1 and RUNX2 deletion mutants were assessed by PLA The detected interaction sites are marked by fluorescent dots (red); nuclei were counterstained with 4′,6′-diamidino-2-phenylindole (DAPI; blue).

A

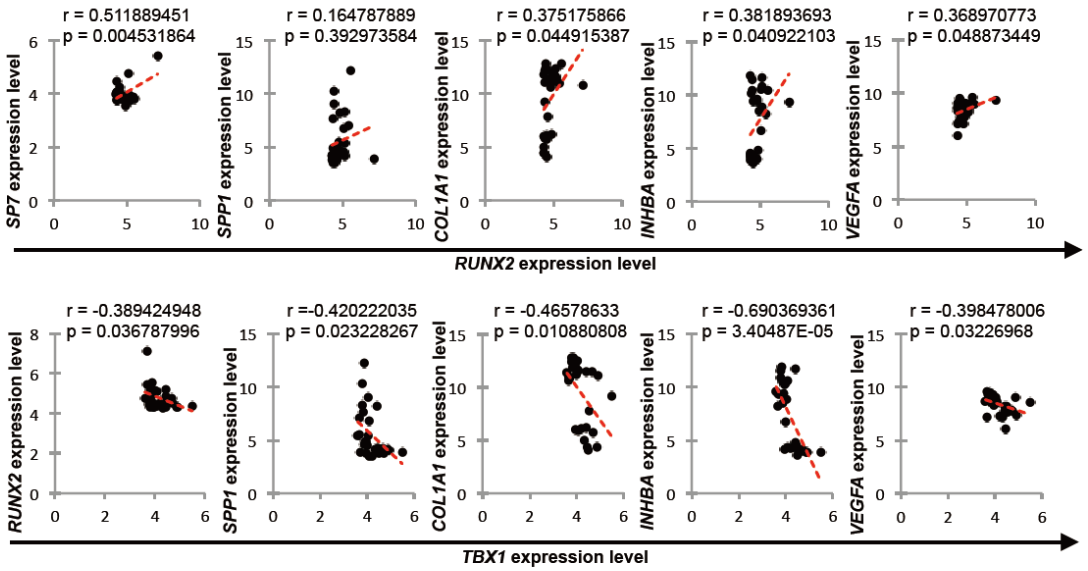

B

		Correlation with *RUNX2* expression				Correlation with *TBX1* expression		
Gene	**Protein**	**r (Pearson)**	***P* value**	***P* value summary**		**r (Pearson)**	***P* value**	***P* value summary**
RUNX2	runt related transcription factor 2	n/a	n/a	n/a		-0.38942	0.036787996	*
SP7	Sp7 transcription factor	0.511889451	0.004531864	**		-0.67566843	0.504997557	ns
SPP1	secreted phosphoprotein 1	0.164787889	0.392973584	ns		-0.42022	0.023228267	*
COL1A1	collagen, type I, alpha-1	0.375175866	0.044915387	*		-0.46578	0.010880808	*
INHBA	inhibin, beta A	0.381893693	0.040922103	*		-0.69036	3.40E-05	***
VEGFA	vascular endothelial growth factor A	0.368970773	0.048873449	*		-0.398478006	0.03226968	*

Appendix Figure 4. TBX1 Negatively Correlates with RUNX2 Target Gene Expression.
(A) Pearson's correlation coefficient. Significant positive correlations between the mRNA expression of *RUNX2* and RUNX2 target genes (upper panels) in bone cell lines from the cancer cell line encyclopedia (CCLE). Conversely, significant negative correlations between mRNA expression levels of *TBX1* and these genes (lower panels).
(B) Correlation with *RUNX2* or *TBX1* and RUNX2 target gene expression in human bone cell lines. Statistical significance is presented as follows: *$P \leq 0.05$; ** $P \leq 0.005$; *** $P \leq 0.0005$; ns; not significant; n/a, not available.

A

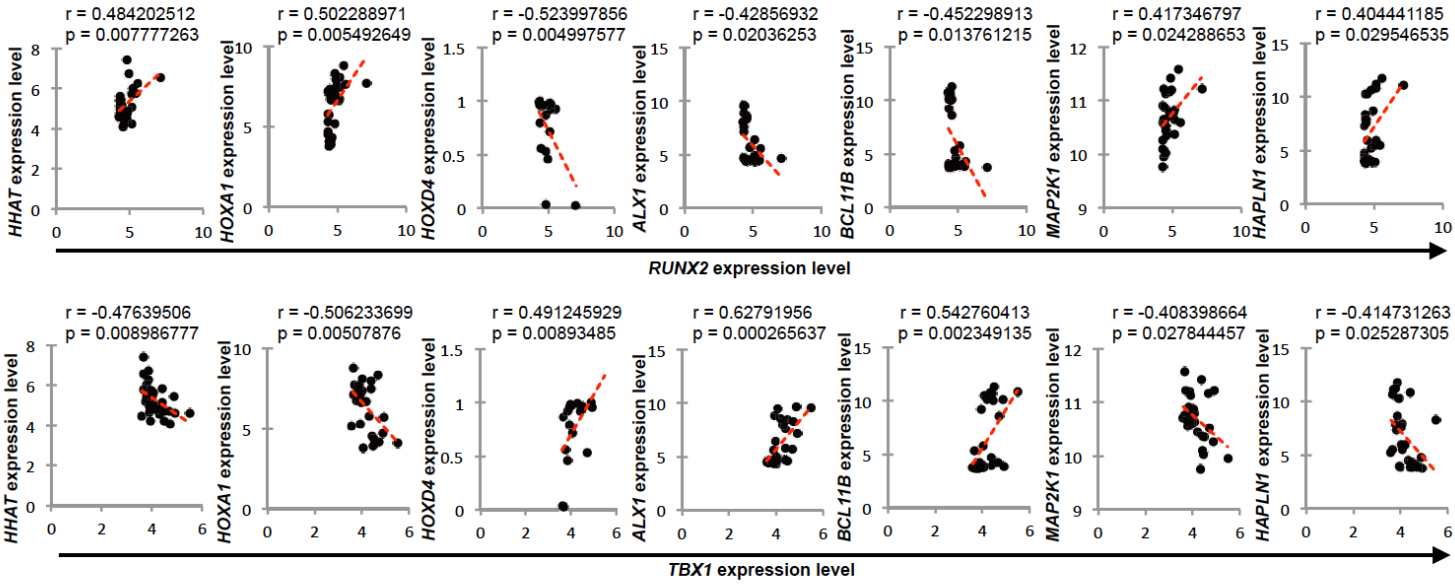

B

		Correlation with *RUNX2* expression			Correlation with *TBX1* expression		
Gene	**Protein**	**r (Pearson)**	***P* value**	***P* value summary**	**r (Pearson)**	***P* value**	***P* value summary**
HHAT	hedgehog acyltransferase	0.484202512	0.007777263	*	-0.47639506	0.008986777	*
HOXA1	homeobox A1	0.502288971	0.005492649	*	-0.506233699	0.00507876	*
HOXD4	homeobox D4	-0.523997856	0.004997577	**	0.491245929	0.00893485	*
ALX1	aristaless-like homeobox 1	-0.42856932	0.02036253	*	0.62791956	0.000265637	***
BCL11B	BAF chromatin remodeling complex subunit BCL11B	-0.452298913	0.013761215	*	0.542760413	0.002349135	**
MAP2K1	mitogen-activated protein kinase kinase 1	0.417346797	0.024288653	*	-0.408398664	0.027844457	*
HAPLN1	hyaluronan and proteoglycan link protein 1	0.404441185	0.029546535	*	-0.414731263	0.025287305	*

Appendix Figure 5. Correlation with *RUNX2* or *TBX1* and Genes Associated with Abnormal Cranial Base Morphology.
(A) Pearson's correlation coefficient. Significant positive correlations between mRNA expression levels of *RUNX2* and genes associated with abnormal cranial base morphology, namely *HHAT, HOXA1*, *MAP2K1*, or *HAPLN1*, in bone cell lines from cancer cell line encyclopedia (CCLE) (upper panels). Conversely, significant negative correlations between mRNA expression levels of *TBX1* and these genes (lower panels).
(B) Correlation with *RUNX2* or *TBX1* and genes associated with abnormal cranial base morphology in human bone cell lines. Genes with statistically significant correlations are shown. Statistical significance is presented as follows: *$P \leq 0.05$; ** $P \leq 0.005$; *** $P \leq 0.0005$.

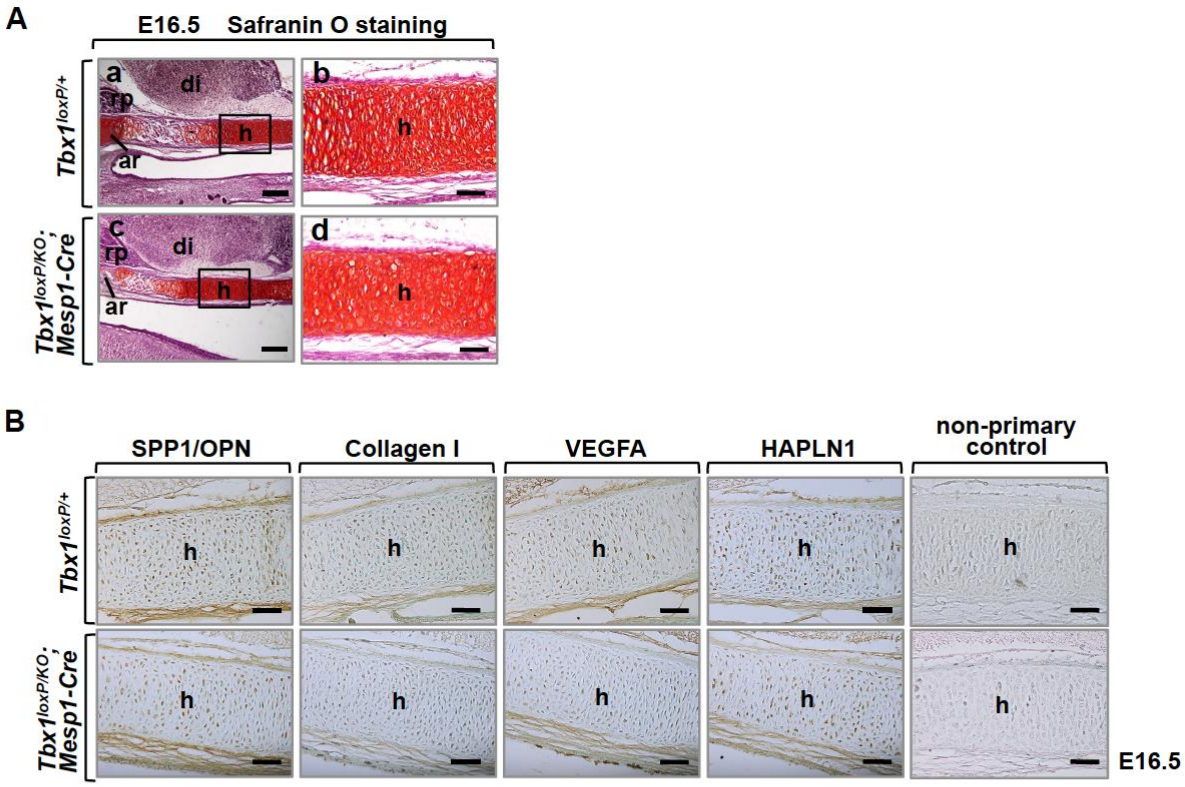

Appendix Figure 6. No difference in chondrocyte differentiation was observed between control and *Tbx1*-deficient hypophyseal cartilage.

(A) Sagittal section of E16.5 control (a,b) and *Tbx1$^{loxP/KO}$; Mesp1-Cre* embryos (c,d) stained with Safranin O/fast green/hematoxylin. (**b,d**) Higher-magnification views of (a) and (c), respectively. ar, acrochordal cartilage; h, hypophyseal cartilage; rp, Rathke's pouch; di, diencephalon. Scale bars: a,c, 200 μm; b,d, 50 μm.

(B) Immunohistochemistry of the cartilage primordium of the intersphenoid synchondrosis for SPP1, Collagen I, VEGFA, and HAPLN1 on sagittal sections of control and *Tbx1$^{loxP/KO}$; Mesp1-Cre* embryos at E16.5. h, hypophyseal cartilage. Scale bars: 50 μm.